Basis for Tubular Joint Design

Design criteria of the codes that govern construction of offshore drilling platforms are analyzed and evaluated

BY P. W. MARSHALL AND A. A. TOPRAC

Introduction

Recently published codes (Refs. 1,2) include criteria for the design and construction of welded connections for circular tubes, which have been in use for a number of years in offshore drilling platforms. The purpose of this paper is to document the background data underlying these criteria, in terms of static and fatigue strength.

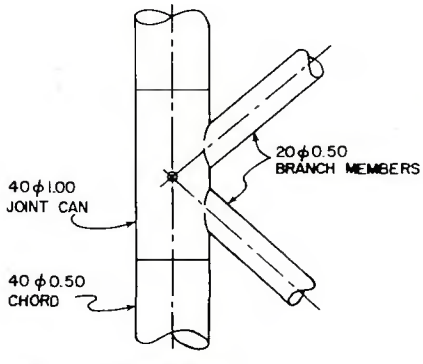

Fig. 1 — Simple joint

P. W. MARSHALL is Staff Civil Engineer, Offshore Construction, Shell Oil Company, New Orleans, La. A. A. TOPRAC is Professor of Civil Engineering, The University of Texas at Austin.

Paper is based on a survey sponsored by the WRC Subcommittee on Welded Tubular Structures.

Static Strength

Simple and Punching Shear Joints

Currently the most popular style of welded connection for intersecting circular tubes as used in fixed offshore structures is the "simple" joint illustrated in Fig. 1. The tubular members are simply welded together, and all load is transferred from one branch to the other via the chord, without any help from stiffening rings or gusset plates. To prevent excessively high localized stresses in the chord, a short length of heavier section (joint can) is often used in the connection area. In such cases, the problem of joint design reduces to that of sizing the joint can, particularly where complete joint penetration groove welds (as defined for tubular structures (Ref. 2) are used at the ends of the branch members.

Although the complete stress picture is much more complex, the concept of punching shear, Fig. 2, has been quite useful in correlating test data and formulating design criteria. The average (or nominal) punching shear stress, v_p, acting on the potential failure surface is calculated as:

$$v_p = \tau\left(\frac{f_a \sin\theta}{k_a} + \frac{f_b}{k_b}\right) \qquad (1)$$

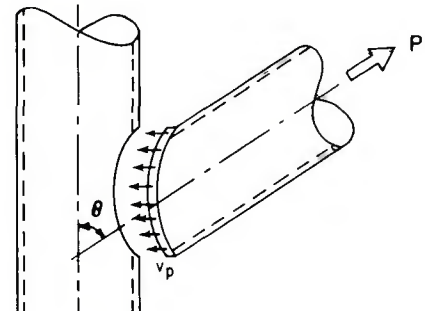

Fig. 2 — Punching shear

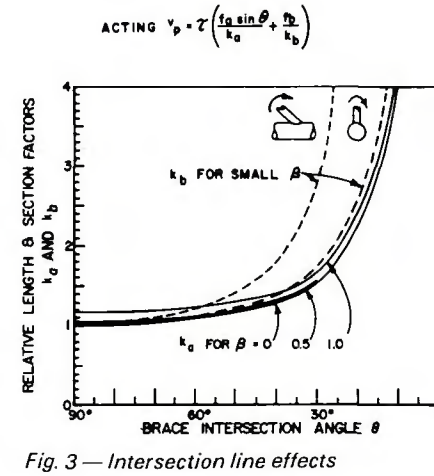

Fig. 3 — Intersection line effects

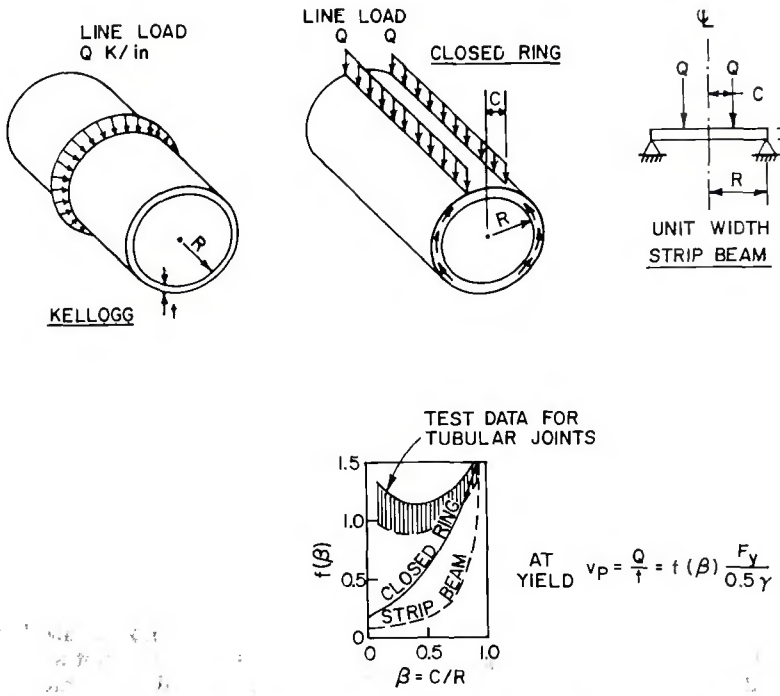

Fig. 4 — Simplified punching shear criteria

Table 1 — Closed Ring and Kellogg Solutions for Punching Shear and Line Load Capacities

Case	Closed ring	Kellogg
Punching shear capacity	$v_p = \frac{F_y}{0.5\gamma} \times f(\beta)$	$v_p = \frac{F_y}{2.34 \times \gamma^{0.5}}$
Total joint capacity proportional to	$t^2 \times \text{length} \times f(\beta)$	$t^{1.5} \times \text{perimeter}$

where $\tau = t_b/t$ = ratio of branch thickness to chord thickness,

θ = angle between member axes (see Fig. 2),

f_a and f_b = nominal axial and bending stresses in branch, respectively.

It is to be noted that only the component of the branch member load which is perpendicular to the main member (chord) wall is considered because this component is responsible for most of the localized stresses. The terms K_a and k_b relate to the length and section modulus, respectively, of the tube-to-tube intersection, which is kind of a saddle-shaped oval (Ref. 3). Specifically the terms represent the ratio of the true perimeter (or section modulus) to that of the circular brace; they are plotted in Fig. 3, as a function of θ (defined above) and β, where

$\beta = \frac{R_b}{R}$ = brace to chord diameter (or radius) ratio

To specify design allowable values for the punching shear stress theoretical and experimental considerations are discussed below.

Theoretical Approach. Solutions for elastic stresses in cylindrical shells subjected to localized line loads are available for the very simple load cases shown in Fig. 4. The closed ring solution and Kellogg formula (Ref. 4) indicate punching shear and line load capacities as shown in Table 1.

Note that punching shear capacity is defined in relation to the very important nondimensional parameter γ where

$\gamma = R/t$ = chord thinness ratio, radius/thickness

This is analogous to the span to depth ratio of a strip beam, for which similar relationships may be derived (see Fig. 4).

These two relatively crude physical models might be expected to bracket the behavior of simple tubular joints, since the branch member loads the chord along a combination of longitudinal and circumferential lines. Unfortunately they yield divergent results and tend to indicate disturbingly high stresses in practical design situations. However, they both do reflect the strong dependence of total joint capacity on chord thickness and branch member perimeter. The additional effect of diameter ratio, $f(\beta)$, as indicated by Roark, was considered paradoxical in that test data with tubular connections did not show the same monotonic increase in joint efficiency as depicted in Fig. 4. In fact, T-joint tests cited by Toprac (Ref. 4) showed joint efficiency (in terms of the ratio of hot spot stress to punching shear) passing through a minimum in the midrange of diameter ratios.

A sophisticated analytical solution (Ref. 5) yields the more realistic picture presented in Fig. 5. These results are consistent with those obtained experimentally and with finite element analyses (Ref. 6), insofar as stress levels in the chord and load transfer across the weld (Q) are concerned. For this joint, the stress concentration factor is 7.3, and the calculated average punching shear stress, v_p, at which first yield at the hot spot occurs (F_y = 36 ksi) is only 2.5 ksi. Comparable punching shears for Roark and Kellogg would be 2.2 ksi and 3.4 ksi, respectively.

Figure 6 summarizes the results of a parameter study made with computer programs based on Ref. 5. The punching shear stress, v_p, at which yield stress is predicted for axially loaded T-connections, is presented as a function of chord thinness ratio, γ, and brace/chord diameter ratio, β. As was previously noted experimentally, joint efficiency (in terms of punching shear at yield) passes through a miminum for a diameter ratio in the range of 0.4 to 0.7. Throughout this range, punching shear efficiency is more or less independent of diameter ratio, but varies inversely with the 0.7 power of chord thinness ratio γ.

Correspondingly, the overall capacity of the connection would be proportional to the product of brace perimeter (or intersection length) and $t^{1.7}$, where t is chord thickness — a result which is surprisingly consistent with the oversimplified approaches considered earlier.

However, the use of first yield as a failure criterion shows that elastic theories seriously underpredict the available static strength of practical tubular connections. For example, a mild steel scale model of the connection in Fig. 5 actually carried the load shown (appropriately scaled down). Naturally, a hot spot stress of 160 ksi for mild steel is unrealistic and the material is beyond yield, and subjected to strains in excess of 5300 μ in./in. Under these circumstances, it appears that theoretical elastic analyses will be of limited use in formulating practical design criteria for static or quasi-static loading conditions.

Empirical Approach. Tubular joints have a tremendous reserve capacity beyond the point of first yield (Ref. 7),

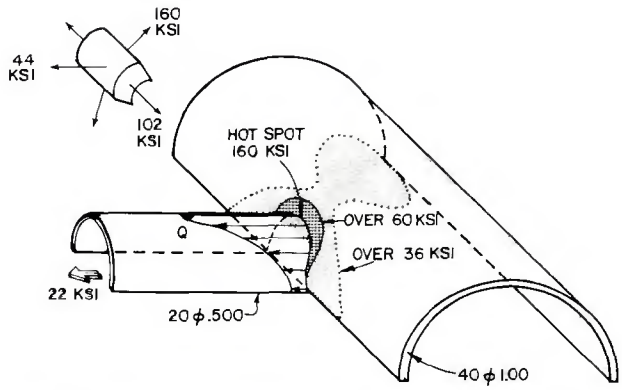

Fig. 5 — Theoretical elastic stresses — axially loaded T-joint

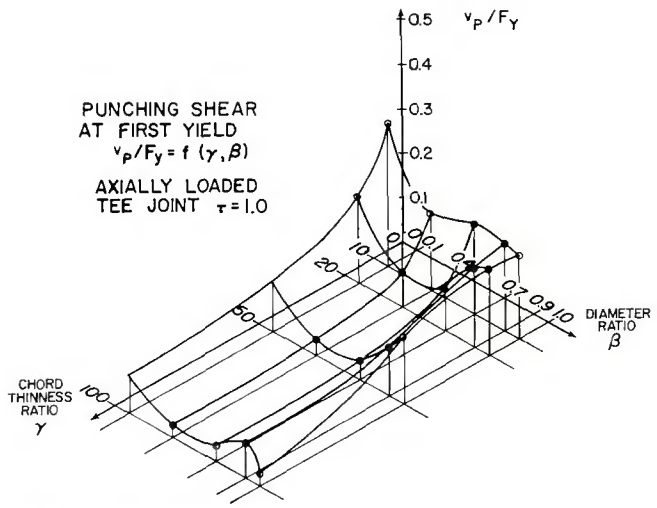

Fig. 6 — Parameter study

as illustrated in Fig. 7. If a section through the chord at its intersection with the brace is considered for small loads in the elastic range, the distribution of circumferential stresses on the outside surface are shown as Stage 1 in the figure. Beyond yield, the connection deforms (Stage 2) while the applied load continues to increase. Finally, at loads 2.5 to 8 times that at first yield, the joint fails — by pullout failure as shown for tension loads or by localized collapse of the chord for compression loads (Stage 3).

The average punching shear stress at failure*, v_p, has been plotted in Fig. 8 relative to specified minimum yield strength, F_y, and as a function of chord thinness ratio, γ; 38 static tests which failed in the punching shear mode are represented, along with two specimens which failed after only a few cycles of fatigue loading. The solid circles represent K-joints; the rest are T and cross joints. Data are from Toprac (Refs. 4, 7) and other sources (Refs. 8, 9).

For relatively stocky chord members — thickness greater than 7% of diameter or γ less than 7 — the joints may be said to have a 100% punching shear efficiency, in the sense that the shear strength of the material is fully mobilized on the potential failure surface. This criterion is met by ASTM A-53 standard weight pipe under 2 in. diam, by extra strong pipe under 5 in. diam, and by double extra strong pipe through 12 in. diam.

Larger and/or thinner chords should be treated on the basis of a reduced punching shear capacity as given by the curve in Fig. 8 and

$$\text{Ultimate } v_p = \frac{F_y}{0.5 \times \gamma^{0.7}} \qquad (2)^{**}$$

$$\text{Allowable } v_p = \frac{F_y}{0.9 \times \gamma^{0.7}} \qquad (2a)$$

Here, the design allowable punching shear stress incorporates a safety factor of 1.8 with respect to the empirical curve for ultimate punching shear. Its intended range of application is for the mid-range of diameter ratios for which v_p is more or less independent of β.

Since the proposed empirical design curve makes use of the post-yield reserve strength of simple tubular connections, it will be instructive to review the sources of this extra capacity. These are:

1. The difference between elastic and plastic bending strength (localized) of the cylindrical shell, a factor of 1.5.
2. Restraint to plastic flow caused by triaxial stresses at the hot spot, a factor of 1.6 for the situation of Fig. 5.
3. Strain hardening — for the mild steels represented in the test data, the ultimate tensile strength (which is at least locally utilized when a joint fails by separation of the material) is greater than the specified minimum yield strength, F_y, (which is used for the empirical correlation and design formula) by factors from 1.6 to 2.4. Correspondingly, it is suggested that F_y used in calculating the allowable v_p should not exceed two-thirds (2/3) the tensile strength.
4. Further increases in capacity result from the redistribution of load, which occurs as the connection yields and approaches its limit load. If the cylindrical shell is visualized as a network of rings and stringers, the sequence of events may occur as illustrated in Fig. 9.

Plastic behavior, triaxial stresses, strain hardening, load redistribution and large deformation behavior place extraordinary demands on the ductility of the chord material. Some localized yielding will occur at design load levels. These considerations should be kept in mind when selecting steels for tubular structures (Ref. 8).

Further Refinements

By and large, design codes represent a consensus of engineering practices in a particular field. There was a general feeling that, while the data of Fig. 8 (as replotted in terms of β in Fig. 10) did not justify taking diameter ratio β into account, experience indicated a beneficial effect as the diameter ratio approaches unity, as indicated by the heavy dashed line in Fig. 10.

Square Tubes. Considerable insight into the effect of β on the ultimate

---

** Failure was defined as first crack for tension loads. This would functionally impair the joint for subsequent fatigue service.*

*** The ultimate strength criteria developed by Reber (Ref. 9) reduces to:*

$$\text{Ultimate } v_p = f(\beta)\frac{F_y}{0.55 \times \gamma^{0.6}}$$

All simple T, Y and K connections are tested on a common basis. Although K connections have lower elastic stresses than the corresponding T and Y connections, they also have less reserve strength, so that the ultimate capacities come out similar. The chief difference between Reber's results and equation (2) is in the degree of conservatism with respect to the scatter band shown by the test results. Reber provides a good average fit whereas the curve for equation (2) falls on the safe side of most of the data. Reber's $f(\beta)$ shows relatively little influence of diameter ratio: i.e., $f(\beta) = \beta^{0.1}$

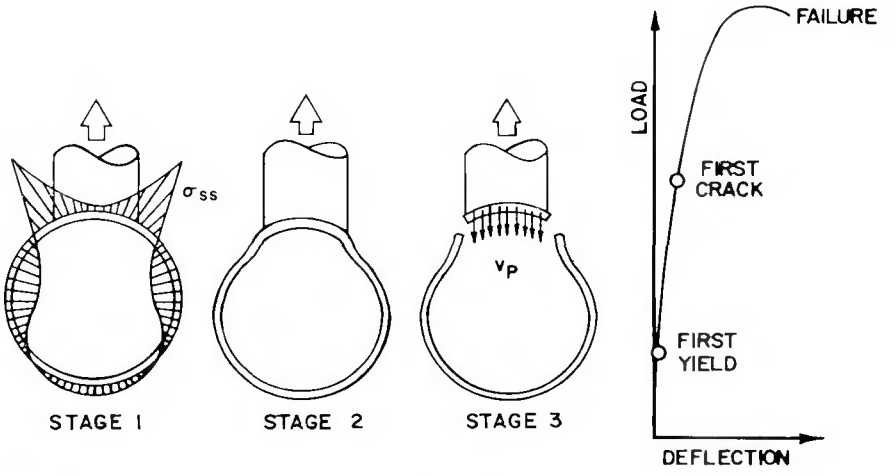

Fig. 7 — Reserve strength of a tubular connection

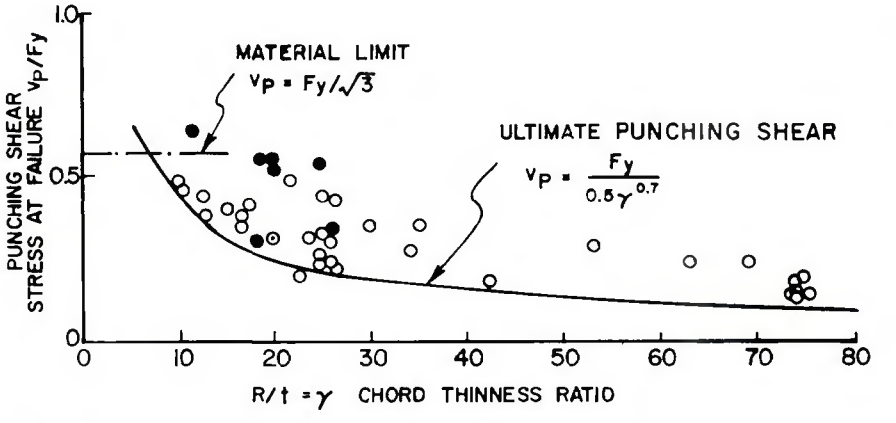

Fig. 8 — Empirical design curve — static strength

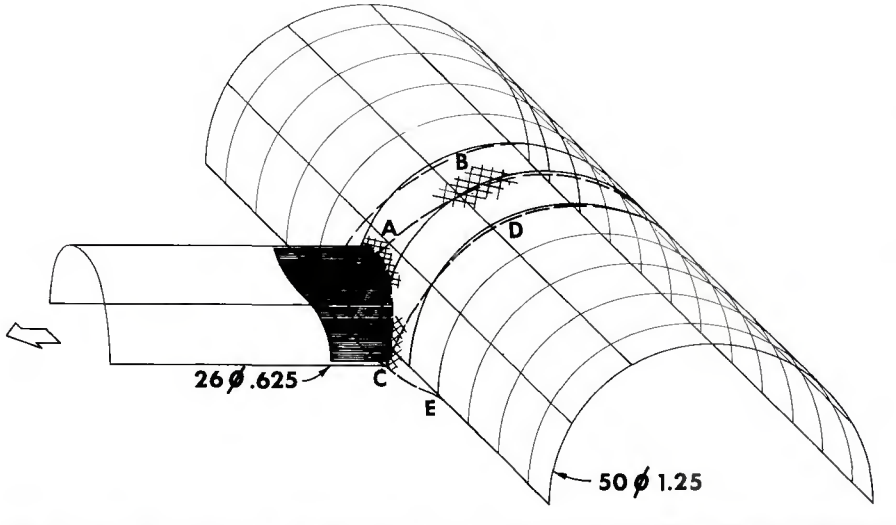

Fig. 9 — Load redistribution. First yielding occurs at hot spot A. Cross hatched yield line is analogous to plastic hinge in a continuous frame. Full strength of ring AB is reached when yielding also occurs at B, after considerable angle change at hot spot. Ring AB continues to deform at constant load while rest of joint catches up, resulting in more uniform load distribution. Limit load of joint is reached when ring CD and stringer CE also yield. Deformed shape is indicated by dashed lines

punching shear capacity of tubular connections was gained from consideration of a limit analysis of square tubes. Using the yield line pattern of Fig. 11 and the upper bound theorem of plastic design, the ultimate punching shear stress v_p is obtained as:

$$v_p = \frac{0.25}{\beta(1-\beta)} \cdot \frac{F_y}{0.5 \times \gamma^{1.0}} \qquad (3)$$

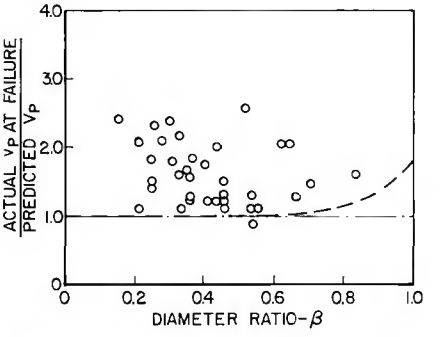

Fig. 10 — Static strength — β effects

where β and γ are defined in a manner analogous to the usage for circular tubes.

The second term on the right of equation (3) is quite similar to the empirical punching shear, equation (2); only the exponent of γ is different. The leading term corresponds to the β effect and has the following properties:

1. Minimum value of 1.0, which occurs at $\beta = 0.5$.
2. Increasing punching shear efficiency at larger and smaller β -ratios; this is comparable to the theoretical results for circular T-joints, Fig. 6.
3. Where β approaches its limits (0 and 1.0), punching shear is limited by the shear strength of the material (or by other considerations such as web crippling).

Test data (Ref. 10) for the specific case of 5 × 5 × 0.187 chord are also plotted in Fig. 11. Failure was defined as when joint deformation reached 3% of chord width. The strength increase for β -ratios over 0.5 appears to be confirmed, with the test data showing strengths ranging from 1.5 to 1.8 times the computed "upper bound" limit load. This reserve strength undoubtedly comes from some of the same sources discussed above for circular tube connections.

For β -ratios under 0.5, however, the test data show equation (3) to be increasingly less conservative as β decreases. The dotted line (Fig. 11) represents a punching shear criteria which is independent of the β -ratio, given by:

$$v_p = \frac{F_y}{0.5\,\gamma} \quad \text{for } \beta < 0.5 \qquad (3a)$$

Note that this straight sloping line goes through the origin; total joint capacity goes to zero as the brace perimeter and β -ratio also approach zero. The combination of equations (3) and (3a) results in criteria with more or less consistent safety factors throughout the range of β.

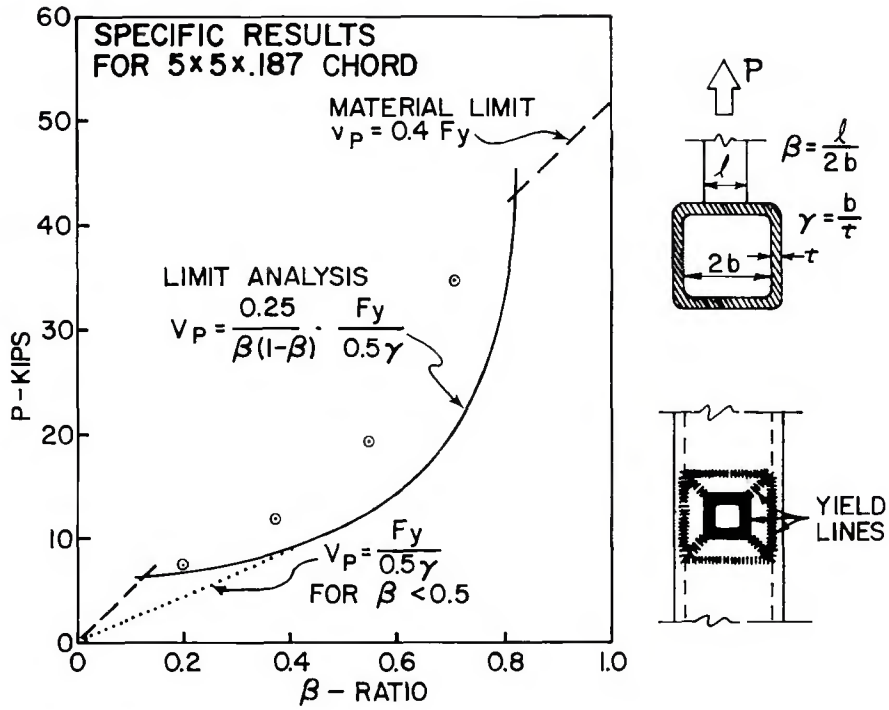

Fig. 11 — Ultimate strength analysis — square tubes

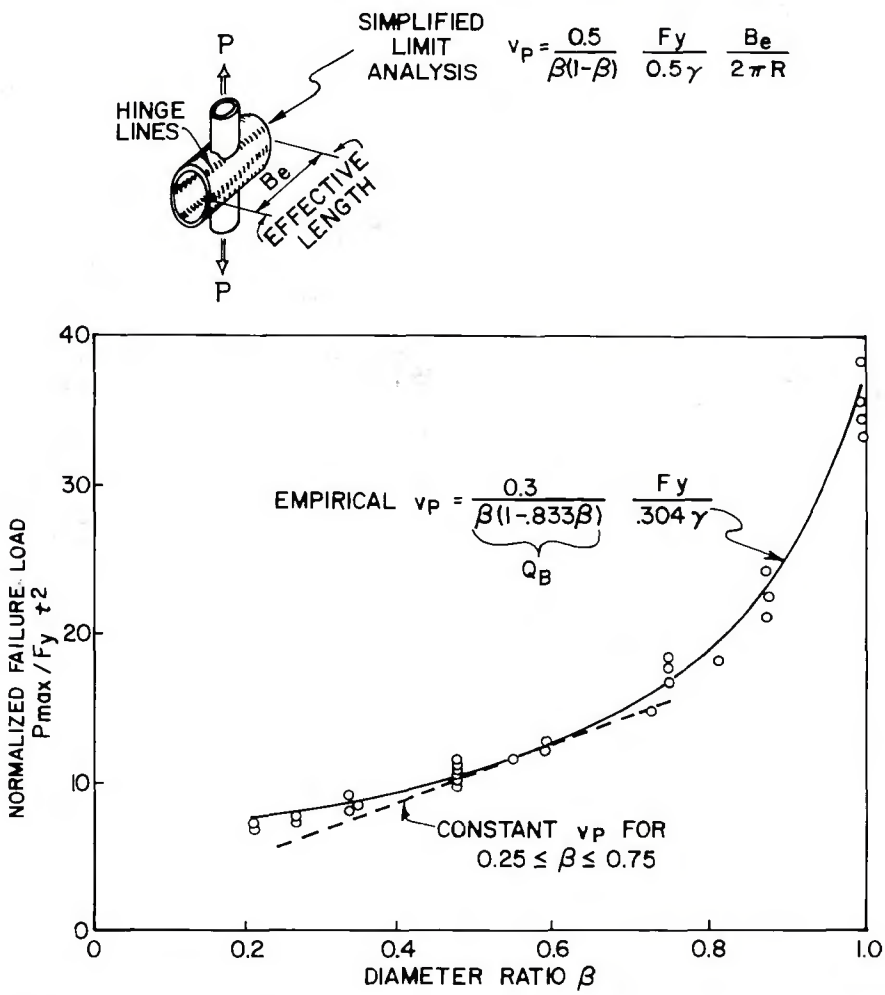

Fig. 12 — Japanese results — cross joints

Japanese Research

A simplified limit analysis of cross joints with circular tubes has been reported (Ref. 11), which employs the physical model of Fig. 12 to derive an expression for theoretical ultimate strength which can be reduced to the following:

$$v_p = \frac{0.5}{\beta(1-\beta)} \cdot \frac{F_y}{0.5\gamma} \cdot \frac{B_e}{2\pi R} \quad (4)$$

When the effective length B_e is taken as equal to the chord circumference, the last term becomes unity, and equation (4) becomes identical with equation (3), with a term for the basic variation of v_p with F_y and γ, modified by a term expressing the β -effect.

Test data were used to justify an empirical modification of the expression for ultimate punching shear, leading to the results plotted in Fig. 12, and

$$v_p = \frac{0.3}{\beta(1-0.833\beta)} \cdot \frac{F_y}{0.304\gamma} \quad (4a)$$

In this expression the term for β -effect has the following properties and implications:

1. A value of 1.0 for $\beta = 0.6$
2. Increasing joint efficiency for larger β -ratios, up to a limiting increase of 1.8-fold for $\beta = 1.0$.

Note that for the mid-range of diameter ratios (β from 0.25 to 0.75) the assumption of constant punching shear also provides a reasonable fit to the data of Fig. 12, in line with earlier results. For very small β-ratios, there is little experimental justification for the large increases in joint efficiency predicted by the β -modifier in equation (4a). Accordingly, it has been recommended that a modifier of unity be used for values of β less than 0.6. This is consistent with the results for square tubes, and appears to be conservative with respect to theoretical results (Fig. 6).

Proposed β-Effect

Applying the modifier, Q_β, for the effects of diameter ratio, to the punching shear criteria of equations proposed earlier (equations (2) and (2a) one obtains:

$$\text{Ultimate } v_p = Q_\beta \cdot \frac{F_y}{0.5 \times \gamma^{0.7}} \quad (5)$$

$$\text{Allowable } v_y = Q_\beta \frac{F_y}{0.9 \times \gamma^{0.7}}$$

where

$$Q_\beta = \frac{0.3}{\beta(1-0.833\beta)} \quad \text{for } \beta > 0.6$$

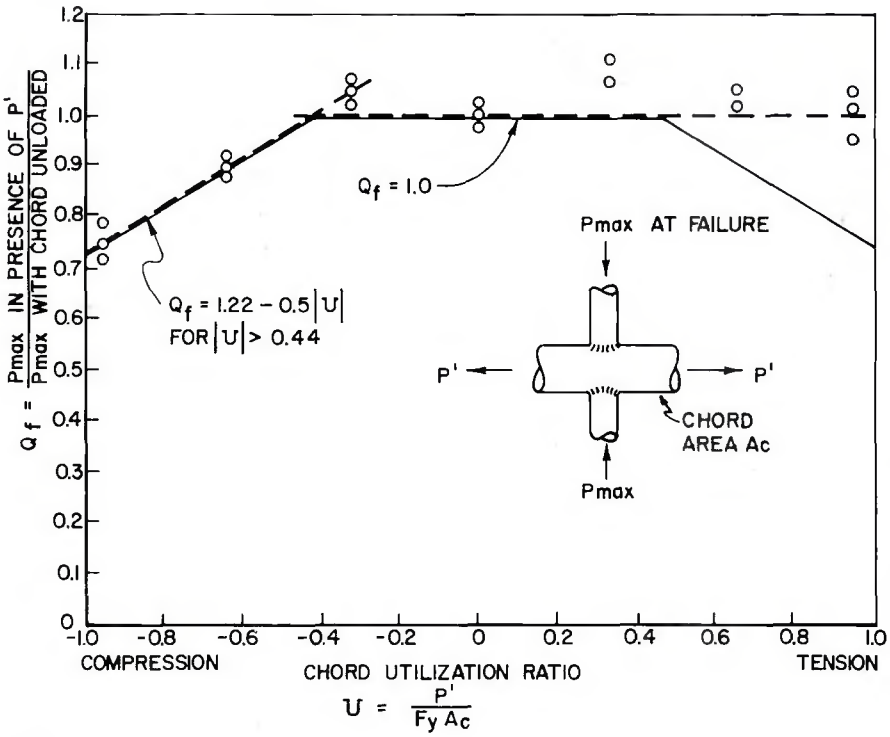

Fig. 13 — Interaction effects of stress in chord

and $Q_\beta = 1.0$ for $\beta \leq 0.6$

These criteria, including Q_β, are plotted as the heavy dashed line in Fig. 10.

Interaction Effects

Japanese data (Ref. 11), showing the extent to which axial load in the chord member reduces its capacity to carry punching shear, are plotted in Fig. 13. The proposed modifier Q_f for interaction effects would be used in design as follows:

$$\text{Allowable } v_p = Q_f \cdot Q_\beta \cdot \frac{F_y}{0.9 \times \gamma^{0.7}} \quad (6)$$

where $Q_f = 1.22 - 0.5|U|$ for $|U| > 0.44$
$Q_f = 1.0$ for $|U| \leq 0.44$

and $|U|$ = chord utilization ratio at the connection.

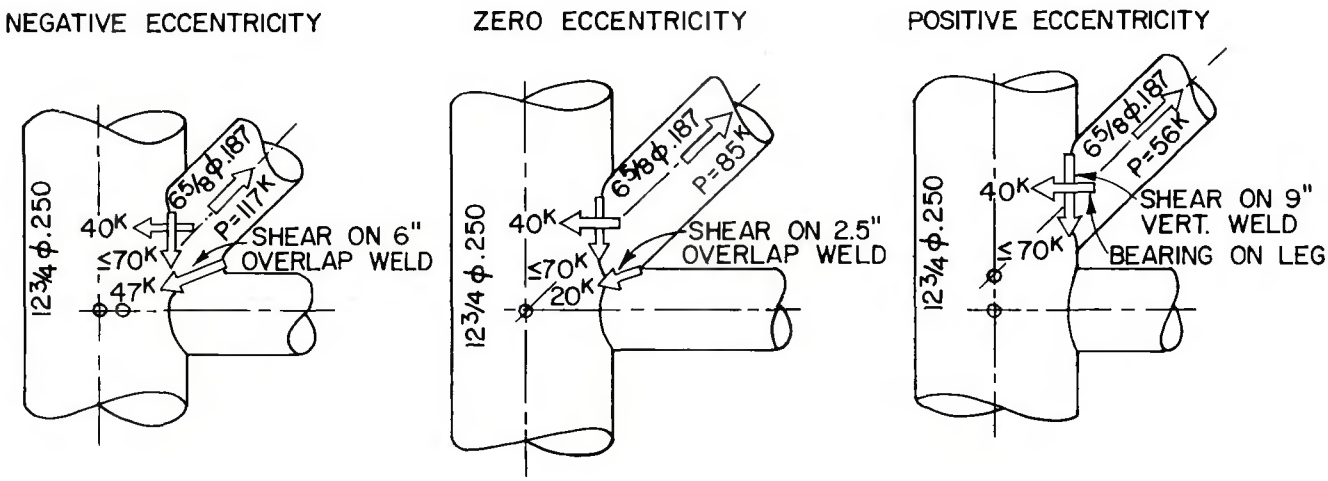

COMPARISON OF JOINT EFFICIENCIES		
TYPE OF JOINT	CALCULATED BASED ON NOM. YIELD 137K IN 6⅝ ϕ	TEST RESULTS BASED ON ULTIMATE 255K IN 6⅝ ϕ
POSITIVE ECCENTRICITY	41%	54%
ZERO ECCENTRICITY	62%	82%
NEGATIVE ECCENTRICITY	86%	108%

Fig. 14 — Joints of various eccentricities

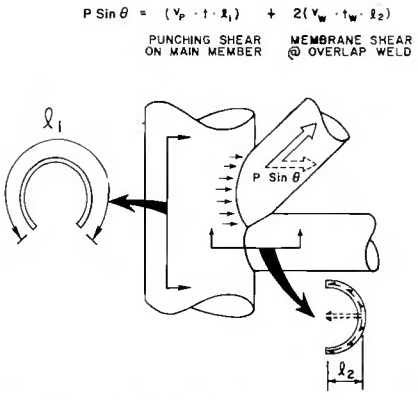

Fig. 15 — Components of resistance for overlapping joints

In design |U| would be taken as the AISC ratio for the chord at the tubular connection (with respect to criteria based on yield). Equation (6) includes safety factors and corresponds to a symmetrical failure envelope, as shown by the solid line (Fig. 13). Where heavy wall joint cans are used at tubular connections, the utilization ratio will often be less than 0.44 for the joint can, corresponding to no reductions due to interaction. For highly stressed K and X-joints without joint cans, but with equal diameters, the increase in joint efficiency over equation (2a) will be limited to about 30%, when both Q_β and Q_f are considered.

Overlapping Joints

In overlapping joints, the braces intersect each other as well as the chord, and part of the load is transferred directly from one brace to another through their common weld. One advantage of such joints is that, since the chord no longer must transfer the entire load, its thickness can be reduced and "joint cans" eliminated. The amount of overlap can be controlled by adjusting the eccentricity of brace centerlines, as indicated in Fig. 14. Negative eccentricity (Ref. 12) can be used to increase the amount of overlap and the static load transfer capacity of the connection.

A crude ultimate strength analysis is proposed (see Fig. 15), in which the punching shear capacity for that portion of the brace reaching the main member and the membrane shear capacity of the common weld between braces are assumed to act simultaneously. Thus, the total capacity of the connection for transferring loads perpendicular to the chord becomes

$$P \sin\theta = v_p t l_1 + 2 v_w t_w l_2 \qquad (7)$$

where

v_p = allowable punching shear stress equation (6) for the main member

t = main member wall thickness

l_1 = circumferential length for that portion of the brace which contacts the main member

and

v_w = allowable shear stress for the common weld between the braces*

t_w = throat thickness for the common weld between braces*

l_2 = the projected chord length (one side) of the overlapping weld, measured in the plane of the braces and perpendicular to the main member**

A comparison of computed capacities, in terms of brace axial load, P, using ultimate v_p and yield $v_w \times t_w$, versus test results is given in Fig. 14. Equation (6) appears to be conservative in predicting static joint capacities, provided there is sufficient ductility that the stiffer element (the overlap) does not fail before the rest of the joint catches up. At elastic load levels the overlap is so much stiffer that it tries to carry the entire load; thus, where overlapping joints are intentionally used, some designers like to proportion the overlap to carry at least 50% of the acting transverse load.

Where extreme amounts of overlap are used, it may become necessary to check the capacity of the connection for transferring loads parallel to the main member as well as transverse loads. Both may be accomplished with vector combination of the various strength elements, as suggested in Figs.14 and 15.

Fatigue

Few members or connections in conventional buildings need to be designed for fatigue, since most load changes occur infrequently or produce only minor cyclic stresses. The full design wind or earthquake loads are sufficiently rare that fatigue need not be considered.

However, crane runways and supporting structures for machinery are often subject to fatigue loading conditions. Offshore structures are subject to a continuous spectrum of cyclic wave loadings, which require consideration of cumulative fatigue damage (Ref. 13).

Welded tubular connections, in particular, require special attention to fatigue, since statically acceptable designs may be subject to localized plastic strains, even at nominally allowable stress levels.

Fatigue may be defined as damage that results in fracture after a suffi-

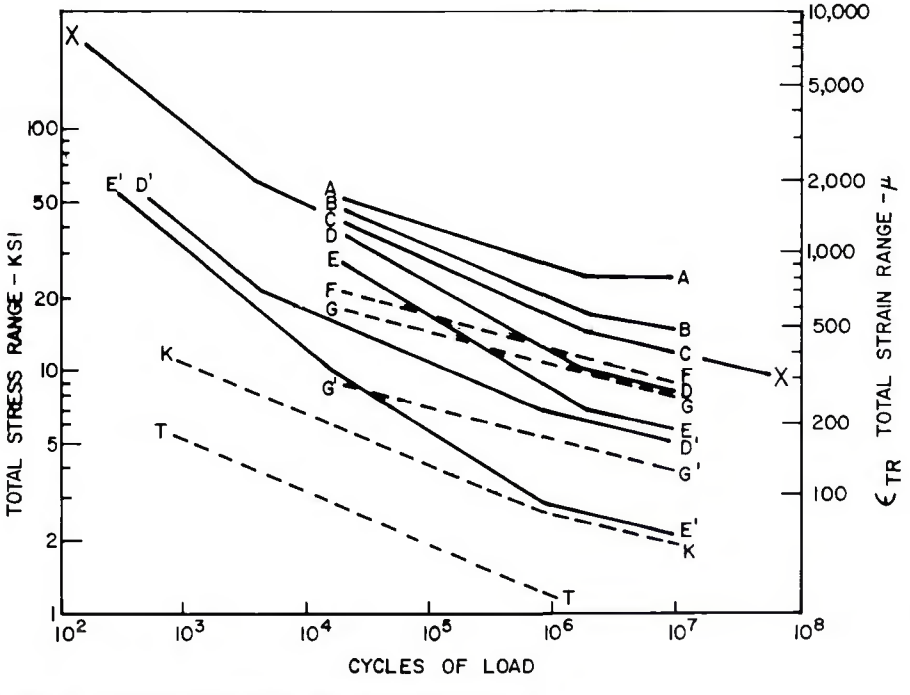

Fig. 16 — Family of fatigue design curves (see Table 1)

**Except that the line load capacity $v_w \times t_w$ should not exceed the shearing capacity of the thinner adjoining base metal.*

***Projected chord length is proportional to the resultant of membrane shear, acting at peak value along the full length of the overlapping weld.*

Table 2 — Fatigue Categories

Stress category	Situation	Kinds of stress[a]
A	Plain unwelded tube.	TCBR
A	Butt splices, no change in section, full penetration groove welds, ground flush, and inspected by x-ray or UT.	TCBR
B	Tube with longitudinal seam.	TCBR
B	Butt splices, full penetration groove welds, ground flush.	TCBR
B	Members with continuously welded longitudinal stiffeners.	TCBR
C	Butt splices, full penetration groove welds, as welded.	TCBR
D	Members with transverse (ring) stiffeners, or miscellaneous attachments such as clips, brackets, etc.	TCBR
D	Tee and cruciform joints with full penetration welds (except at tubular connections).	TCBR
D'[b]	Simple T, Y, or K connections with full penetration tubular groove welds.	TCBR in branch member (main member must be checked separately per Category K or T).
E	Balanced T and cruciform joints with partial penetration groove welds or fillet welds (except at tubular connections).	TCBR in member (weld must also be checked per Category G).
E	Members where doubler wrap, cover plates, longitudinal stiffeners, gusset plates, etc., terminate (except at tubular connections).	TCBR in member.
E'[b]	Simple T, Y, and K type tubular connections with partial penetration groove welds or fillet welds; also complex tubular connections in which load transfer is accomplished by overlap (negative eccentricity,) gusset plates, ring stiffeners, etc.	TCBR in branch member (main member in simple T, Y, or K connections must be checked separately per Category K or T; weld must also be checked per Category G').
F	End weld of cover plate or doubler wrap; welds on gusset plates, stiffeners, etc.	Shear in weld.
G	T and cruciform joints, loaded in tension or bending, having fillet or partial penetration groove welds.	Shear in weld (regardless of direction of loading).
G'	Simple T, Y, or K connections having fillet or partial penetration groove welds.	Nominal shear in weld ($P/A + M/S$)
X	Main member at simple T, Y, and K connection.	Hot spot, stress or strain on the outside surface of the main member, at the toe of weld joining branch member — measured in model of prototype connection, or calculated with best available theory.
X	Unreinforced cone-cylinder intersection.	Hot spot stress at angle change.
X	Connections whose adequacy is determined by testing an accurately scaled steel model.	Worst measured hot spot strain, after shake down.
K[c]	Simple K type tubular connections in which gamma ratio R/T of main member does not exceed 24.	Punching shear on shear area[d] of main member.
T[c]	Simple T and Y tubular connections in which gamma ratio R/T of main member does not exceed 24.	Punching shear on shear area[d] of main member.

(a) T = tension, C = compression, B = bending, R = reversal.
(b, c) Empirical curves based on "typical" connection geometries; if actual stress concentration factors or hot spot strains are known, use of curve X is to be preferred.
(d) Equation 1

cient number of fluctuations of stress. Where the fatigue environment involves stress cycles of varying magnitude and varying numbers of applications, failure is usually assumed to occur (or reach a given probability level) when the cumulative damage ratio, D, reaches unity, where

$$D = \Sigma\, n/N \qquad (8)$$

and n = number of cycles applied at a given stress range

N = number of cycles at that stress range corresponding to failure (or a given probability of failure)

Some designers limit the damage ratio to 0.33 when using median or best fit fatigue curves, corresponding to a safety factor of 3 on computed fatigue life. An alternative approach, which will be presented here, is to use fatigue curves which fall on the safe side of most of the data. It might be noted that a linear cumulative damage rule is consistent with the fracture mechanics approach to fatigue crack propagation (Ref. 14).

Stress fluctuations will be defined in terms of stress range, the peak-to-trough magnitude of these fluctuations. Mean stress is ignored. In welded structures we usually do not know the zero point, as there are residual stresses as high as yield which result from the heat of welding. Where there is localized plastic deformation during shakedown, a new set of residual stresses develop. What is usually measured on the actual structure (or a scale model) is the strain range, with the zero point undefined. The constant strain range approximation is in fair agreement with the results of fatigue tests on practical as-welded joints, particularly in the low cycle range.

Fatigue criteria are presented as a set of S-N design curves (Fig. 16) for the various situations categorized in Table 2.

Curves A, B, C, D, E, F, and G are consistent with AISC fatigue criteria (Ref. 15), which appear in turn to reflect the data published earlier by WRC (Ref. 16). Curves rather than tabulated (step function) allowables

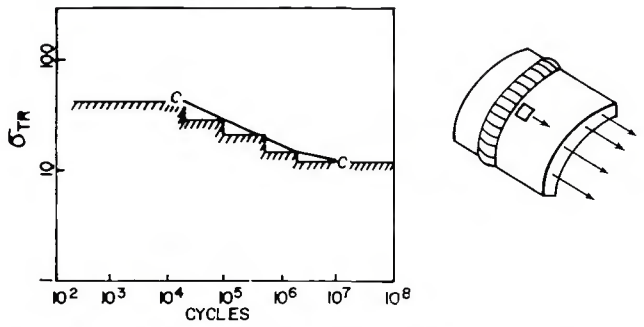

Fig. 17 — Fatigue curve C — nominal stress adjacent to weld

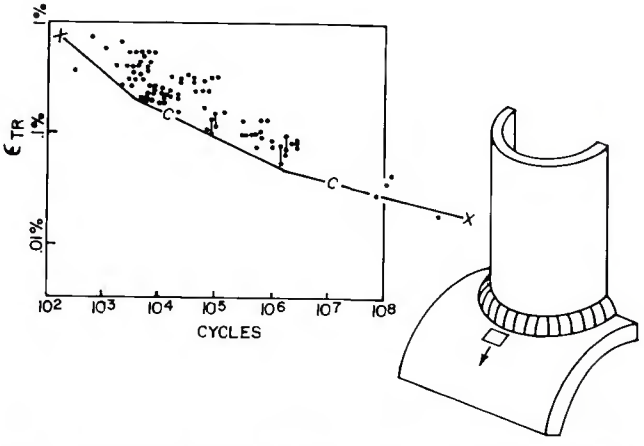

Fig. 18 — Fatigue curves C and X — hot spot strain adjacent to weld

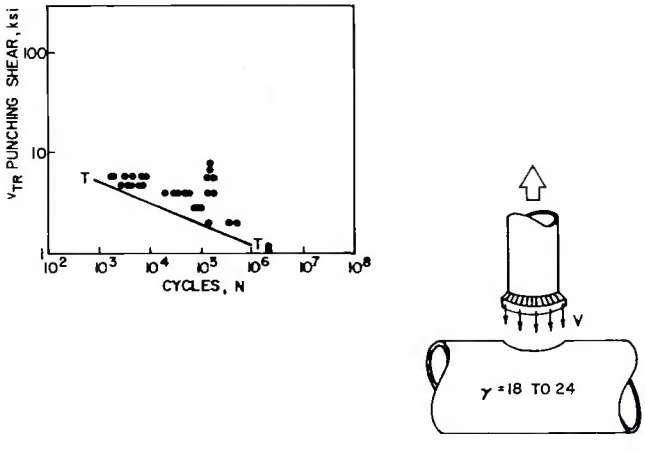

Fig. 19 — Punching shear fatigue strength of T-connections

are used because they are more appropriate to tubular structures exposed to a continuous spectrum of cyclic loads. In these simple situations the nominal member stress ($f_a + f_b$) fairly well represents the actual stress as would be measured adjacent to the weld. See Fig. 17.

Curve X is based on current design practices for offshore structures (Ref. 8). The relevant stress for fatigue failure of tubular connections is the hot spot stress measured adjacent to the weld, as shown in Fig. 18. This is usually considerably higher than the nominal member stress, and would normally be determined from a detailed theoretical (Refs. 5, 6), or experimental (Refs. 4, 7), analysis of the connection. Category X is consistent with category C since the local transverse stress adjacent to the weld is considered in both cases. In the range of inelastic stresses and low cycle fatigue (Ref. 17) it is more realistic to deal in terms of hot spot strain rather than stress.

The data plotted in Fig. 18 represent hot spot stress (or strain) from actual as-welded hardware — tubular connections, pressure vessels, laboratory models and prototype failures — from a variety of sources (Refs. 13, 14, 16, 18, 19, 20, 21). In the low cycle range, the design curve corresponds to roughly 95% survival (5% failure probability) based on test data which are spread out over a scatter band more than one log cycle wide. Within this range, all structural qual-

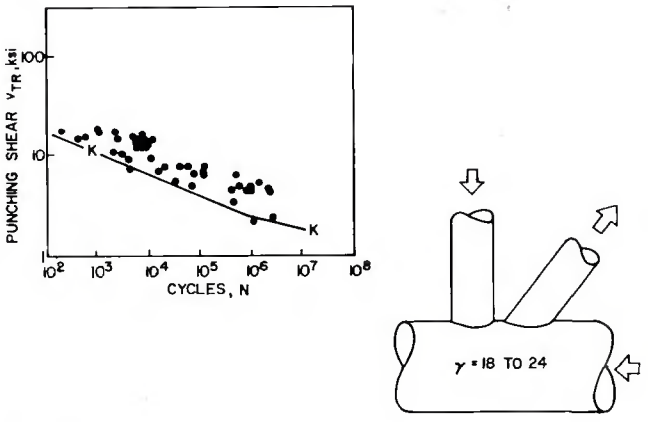

Fig. 20 — Punching shear fatigue strength of K-connections

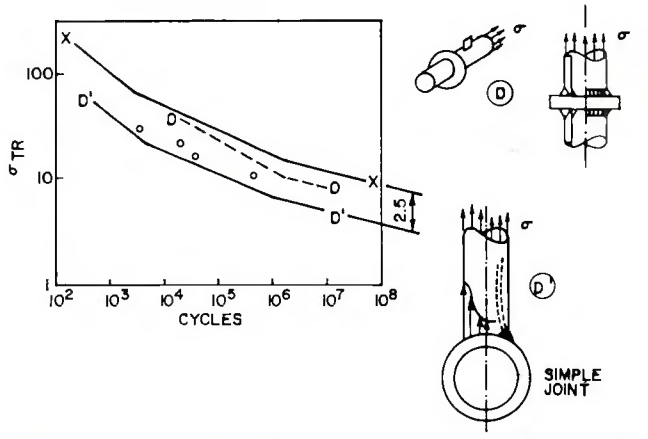

Fig. 21 — Fatigue curves D and D' — nominal member stress at full penetration T welds and simple joints

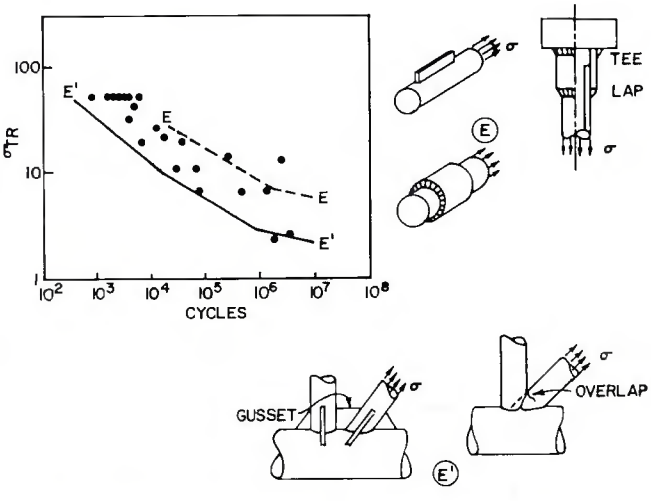

Fig. 22 — Fatigue curves E and E' — nominal member stress at fillet welds and complex joints

ity steels show similar fatigue behavior, independent of yield strength in the range of 36 to 100 ksi: Differences which show up for smooth polished laboratory specimens in the high cycle range simply do not apply to practical as-welded (notched) hardware subjected to localized plastic strains in the presence of a corrosive environment (e.g., seawater).

Little data are available for the high cycle range, over 2×10^6 cycles. In the presence of initial flows and/or corrosive environments, there is no endurance limit, and the fatigue strength continues to drop off.

Unfortunately, use of curve X requires knowledge of stress concentration factors and hot spot stresses within the tubular connections — information which would not be available to many designers. However, anyone should be able to calculate punching shear (equation 1) and make use of the empirical design curves T and K (Figs. 19 and 20) for cyclic punching shear in, respectively, T and K connections. These are based on data assembled by Toprac (Ref. 21) from tests in which the chord thinness ratio, γ , was limited to the range of 18 to 24. Thus the curves may err on the safe side for very heavy chord members (γ under 18), and they could be unconservative for chords with γ over 24. Since the theoretical elastic punching shear efficiency (Fig. 6) varies inversely with $\gamma^{0.7}$, it is suggested that, for chords having γ greater than 24, the allowable cyclic punching shear be reduced in proportion to $(24/\gamma)^{0.7}$.

Once failure of the chord in the punching shear mode has been prevented, by the use of heavy wall "joint cans" or by means of other joint reinforcement, the problem of possible fatigue failure in the braces remains. In simple joints, localized stresses in the brace may reach 2.5 times nominal $f_a + f_b$ due to non-uniform load transfer (a factor of about 2, Fig. 5), restraint to Poisson's-ratio breathing (a factor of 1.6 for perfect axisymmetric restraint), and continuity with the severely deformed chord. Accordingly, curve D' (Fig. 21) when applied to nominal brace stress takes these factors into account. Data points are for thick walled simple joints tested by Bouwkamp et al (Refs. 14, 19), for which failure occurred in the brace (branch member) rather than in the chord (main member).

Where some other form of joint reinforcement is used (such as brace overlap, gussets, or rings) localized stresses in the brace may become larger and more difficult to ascertain and thus have to be designed according to curve E' (Fig. 22), which implies stress concentration factors as high as 6. However, it should be stated also that for some connections of this type curve E is too conservative but unfortunately at this stage no distinction can be made.

Curves D, E, F, and G are limited to situations in which nominal member stresses represent actual load transfer across the weld. Curve G' is shifted down to a factor of 2.0 to account for the uneven distribution of load transfer across the weld at the tube-to-tube intersection (Ref. 5).

The data supporting the empirical design curves, T, K, D', and E' generally show more scatter than the more basic data of Fig. 18, primarily because they neglect some of the relevant factors, and only represent "typical" connection geometries. Where actual stress concentration factors are known, the use of curve X is to be preferred.

Because of the uncertainty and scatter involved, calculated fatigue lives should be taken with a healthy amount of skepticism, and should be viewed more as a design guideline than as an absolute requirement of the code.

Concluding Remarks

The criteria presented have been developed primarily on the basis of research and experience with fixed offshore platforms. These structures are highly redundant, and localized tubular joint failures can occur without leading to collapse of the structure.

One purpose in presenting this paper is to let potential designers of other classes of tubular structures see just how the data fall relative to the proposed criteria, and what the scatter is, so that they may be in a position to evaluate the suitability of the criteria for their particular application.

Also, it is hoped that, as additional data become available, they will be compared against the criteria and data given herein. Such comparison, discussion, and re-examination should eventually lead to a better design.

The authors are indebted to their colleagues in the various API, AWS, WRC, and ASCE task groups concerned with welded tubular structures, whose prodding and comments helped shape the guidelines presented here.

References

1. *API Recommended Practice for Planning, Designing, and Constructing Fixed Offshore Platforms,* API RP 2A, Fourth Edition (1973).

2. *American Welding Society Structural Welding Code,* AWS D1.1-72 (1972).

3. British Standard 449-1959 Appendix C, "Determination of the Length of the Curve of Intersection of a Tube with Another Tube or with a Flat Plate", and British Standard 938-1962, *Spec. for General Requirements for the Metal Arc Welding of Structural Steel Tubes to B.S. 1775.*

4. Toprac, A. A., et al., "Welded Tubular Connections: An Investigation of Stresses in T-Joints" *Welding Journal,* Vol. 45, No. 1, January 1966, Res. Suppl., pp. 1-s to 12-s.

5. Dundrova, V., *Stresses at Intersection of Tubes — Cross and T-Joints,* The University of Texas, S.F.R.L. Technical Report P-550-5 (1966).

6. Greste, Ojars, *A Computer Program for the Analysis of Tubular K-Joints,* University of California Structural Engineering Lab. Report No. 69-19 (1969).

7. Beale, L. A., and Toprac, A. A., *Analysis of In-Plane T, Y and K Welded Tubular Connections,* Welding Research Council Bulletin 125, New York, N.Y., October 1967.

8. Marshall, P. W., et al., "Materials Problems in Offshore Platforms," Offshore Technology Conference Preprint No. OTC 1043 (1969).

9. Reber, J. B., "Ultimate Strength Design of Tubular Joints," Offshore Technology Conference Preprint No. OTC 1664 (1972).

10. Graff, W. J., "Welded Tubular Connections of Rectangular and Circular Hollow Sections," paper for presentation to the Texas Section, ASCE, El Paso, October 8-10, 1970.

11. Toprac, A. A., et al., *Studies on Tubular Joints in Japan — Part I — Review of Research Reports,* report prepared for Welding Research Council, Tubular Structures Committee, September, 1968.

12. Bouwkamp, J. G., *Research on Tubular Connections in Structural Work,* Welding Research Council Bulletin No. 71, 1961.

13. Bell, A. O., and Walker, R. C., "Stresses Experienced by an Offshore Mobile Drilling Unit," Offshore Technology Conference Preprint No. OTC 1440 (1971).

14. Becker, J. F., et al., "Fatigue Failure of Welded Tubular Joints," Offshore Technology Conference Preprint No. OTC 1228 (1970).

15. American Institute of Steel Construction, *Specifications for Design, Fabrication and Erection of Structural Steel for Buildings,* New York, N.Y., February 12, 1969.

16. Munse, W. H., and Grover, L., *Fatigue of Welded Steel Structures,* Welding Research Council, New York, N.Y. 1964.

17. Peterson, R. E., "Fatigue of Metals in Engineering and Design," ASTM Marburg Lecture, 1962.

18. Kooistra, L. F., Lange, E. A., and Pickett, A. G., "Full-Size Pressure Vessel Testing and its Application to Design," ASME Paper 63-Wa-293, 1963.

19. Bouwkamp, J. G., *Tubular Joints Under Static and Alternating Loads,* University of California, Structures and Materials Research Report No. 66-15, Berkeley, June 1966.

20. Toprac, A. A., and Natarajan, M., *An Investigation of Welded Tubular Joints: Progress Report,* International Institute of Welding Comm. XV Doc. XV-265-69, June 1969.

21. Toprac, A. A., *Design Considerations for Welded Tubular Connections,* Report prepared for Welding Research Council, Tubular Structures Committee, December 1970.

1974 Revisions to Structural Welding Code

The 1974 Revisions to Structural Welding Code (AWS D1.1—Rev 2-74) contains the second set of authorized revisions to the Structural Welding Code, D1.1-72. For convenience and overall economy in updating existing copies of the Code, 88 pages of the Code have been reprinted, 59 of which have been revised to incorporate changes. (The remaining pages are not changed but appear on the reverse side of revised pages.)

To fulfill the needs of all Code purchasers, the 1974 revisions are available as a bound book and as individual looseleaf sheets. The bound copies are intended primarily for libraries and others who wish to keep their original copies of the Code, as well as the subsequent revisions, intact. The looseleaf version will be ideal, however, for those Code users who plan to update their present Codes by inserting the revision pages into them.

With the looseleaf pages, the time-consuming process of cutting, pasting, or tearing out will be avoided. To update the Code, old pages are simply removed and the new revised pages inserted in their place. All pages are 8½ in. × 11 in. and are punched for three-hole looseleaf or post binders.

All pages revised for 1974 are listed on the contents page, and all changes in figures and tables are enumerated and described immediately following the contents page. Changes in text material are denoted in bold italics; deleted material is crossed through with double lines. (The 1974 revisions can thus be distinguished from the 1973 revisions which are designated by regular italics and single cross-through lines.) The new pages are printed on blue stock, and pages containing 1974 (and/or 1973) revisions are clearly labeled.

These are the principal changes in Code requirements:

- SMAW fillet welding of studs is now permitted.
- The prequalified status of joints welded by short-circuiting transfer GMAW has been removed.
- Camber tolerances of welded members have been revised.
- SNT qualification of all NDT operators is now required.
- Additions and deletions have been made to the lists of prequalified steels for buildings, bridges, and tubular structures.
- Bridge design criteria relating to fatigue stress have been eliminated.

Prices

D1.1-72 Structural Welding Code	$16.00
D1.1-Rev 1-73 1973 Revisions to Structural Welding Code	$6.00
D1.1-Rev 2-74 1974 Revisions to Structural Welding Code	$6.00

Discounts: 25% to A and B members; 20% to bookstores, public libraries and schools; 15% to C and D members. Send your orders to the American Welding Society, 2501 NW 7th Street, Miami, FL 33125. Florida residents add 4% sales tax. Be sure to specify whether you want a looseleaf or a bound copy.